JOURNAL OF GUIDANCE, CONTROL, AND DYNAMICS
Vol. 20, No. 3, May–June 1997

Neighboring Extremal Control Design Using Error Compensation

Theodore J. Kim*
Sandia National Laboratories, Albuquerque, New Mexico 87106
and
David G. Hull†
University of Texas at Austin, Austin, Texas 78712

Error compensation, which has been used to improve the performance of approximate analytical optimal controls, is extended to neighboring extremal control. The optimal control problem with error compensation is defined, the first variation conditions are linearized about an optimal path to account for perturbations in the initial state and the final constraint manifold, and the neighboring extremal control is derived. A vehicle guidance example demonstrates that the tuning procedure inherent in error compensation moves the performance of the derived control toward that of a numerically determined piecewise-linear optimal control.

Nomenclature

a_i, b_i, c_i	= linearization coefficients for trigonometric functions
C_D	= aerodynamic drag coefficient
C_{D_0}	= zero-lift drag coefficient
C_L^*	= lift coefficient for maximum lift/drag ratio
$\bar{C}_L$	= scaled aerodynamic lift coefficient
$\bar{C}_S$	= scaled aerodynamic side force coefficient
E^*	= maximum lift/drag ratio
$\boldsymbol{e}$	= error compensation control vector
h	= altitude, ft
h_R	= density scale height, ft
M	= tuning parameter matrix
m, n, Q, R, S	= sweep variable matrices
t	= time, s
$\boldsymbol{u}$	= aerodynamic control vector
V	= velocity, ft/s
v	= nondimensional velocity
w	= nondimensional density
X	= downrange distance, nm
$\boldsymbol{x}$	= state vector
Y	= cross-range distance, nm
z	= running variable
α	= sweep variable
γ	= flight-path angle
η	= nondimensional cross range
$\boldsymbol{\lambda}, \boldsymbol{\nu}$	= Lagrange multiplier vectors
ξ	= nondimensional downrange
ρ	= air density, slugs/ft^2
χ	= heading angle
ψ	= final constraint manifold
Ω	= endpoint function
ω	= nondimensional density

Introduction

THE philosophy of optimal guidance is to use the optimal control from the sample point to the desired final point in a sample-and-hold fashion. For optimal guidance to be accepted, the optimal control must be analytical (explicit). To obtain an analytical optimal control, it is necessary to make approximations in the model describing the physical system. Rather than discarding these terms, the approach of error compensation (EC) treats them as bounded controls, which need not be written in terms of a small parameter, a requirement of the Hamilton–Jacobi–Bellman expansion approach.[1] Error compensation applied to approximations in the dynamics has been presented[2] and applied to approximate boundary conditions.[3] If an analytical optimal control cannot be obtained, it is possible to guide the dynamic system in the neighborhood of a reference optimal trajectory using neighboring extremal guidance. The purpose of this paper is to extend error compensation to neighboring extremal (NE) control using the sweep method.[4]

After the theory is derived, it is applied to the descent of a hypersonic glider from a constant-altitude cruise to a fixed point on the ground, a problem that previously has been examined.[5] In fact, this work borrows heavily from Ref. 5, using some of the same approximations, the same guidance scheme, and the same numerical test case. However, the inclusion of the error compensation terms improves the performance of the guidance law and moves the trajectory closer to the numerically determined optimal path.

General EC Problem

The EC approach is to rewrite the system dynamics as

$$\dot{\boldsymbol{x}} = \bar{f}(t, \boldsymbol{x}, \boldsymbol{u}) + \boldsymbol{e}(t) \tag{1}$$

where $\boldsymbol{u}$ is the normal control vector and $\bar{f}$ approximates the true dynamics.[2] The inherent bounds on the EC controls are replaced by penalty terms in the performance index J as

$$J = \chi(t_f, \boldsymbol{x}_f) + \int_{t_0}^{t_f} \left[\mathcal{L}(t, \boldsymbol{x}, \boldsymbol{u}) + \frac{1}{2} \boldsymbol{e}^T M^{-1} \boldsymbol{e} \right] \mathrm{d}t \tag{2}$$

where the matrix M is a diagonal matrix of constants. These constants are tuning parameters that are associated with the EC controls. The tuning parameters are user-selected by tuning the control solution against the true vehicle dynamics during computer simulations of the control law.

The general optimal control problem including EC is written

$$\operatorname*{ext}_{\boldsymbol{e}} \min_{\boldsymbol{u}} J \tag{3}$$

subject to the differential equations, Eq. (1), the initial conditions

$$t_0, \boldsymbol{x}_0 \text{ specified}$$

and the final constraint manifold

$$\psi(t_f, \boldsymbol{x}_f) = 0$$

Received June 20, 1995; presented as Paper 95-3289 at the AIAA Guidance, Navigation, and Control Conference, Baltimore, MD, Aug. 7–10, 1995; revision received Feb. 3, 1997; accepted for publication Feb. 4, 1997.

*Senior Member, Technical Staff, Aided Navigation and Remote Sensing Department. Senior Member AIAA.

†M. J. Thompson Regents Professor, Department of Aerospace Engineering and Engineering Mechanics. Associate Fellow AIAA.

The nonstandard notation ext is used because the EC controls extremize (either minimize or maximize) the performance index.

The Bolza function and the Hamiltonian for this problem are

$$G = \chi(t_f, \boldsymbol{x}_f) + \boldsymbol{\nu}^T \psi(t_f, \boldsymbol{x}_f) \tag{4}$$

$$H = \mathcal{L}(t, \boldsymbol{x}, \boldsymbol{u}) + \tfrac{1}{2}\boldsymbol{e}^T M^{-1} \boldsymbol{e} + \boldsymbol{\lambda}^T [\bar{\boldsymbol{f}}(t, \boldsymbol{x}, \boldsymbol{u}) + \boldsymbol{e}] \tag{5}$$

where $\bar{\boldsymbol{f}}$ is the approximate state vector. The Hamiltonian is separable in $\boldsymbol{u}$ and $\boldsymbol{e}$ by definition of the EC controls. If $\chi(t_f, \boldsymbol{x}_f)$ is sufficiently simple so that the performance index is separable in $\boldsymbol{u}$ and $\boldsymbol{e}$, the control solution is independent of the order of optimization.[6] The first variation conditions that describe the extremal path are[2]

$$\frac{\mathrm{d}x}{\mathrm{d}t} = \bar{\boldsymbol{f}}(t, \boldsymbol{x}, \boldsymbol{u}) + \boldsymbol{e}(t) \tag{6}$$

$$\frac{\mathrm{d}\boldsymbol{\lambda}}{\mathrm{d}t} = -H_{\boldsymbol{x}}^T(t, \boldsymbol{x}, \boldsymbol{u}, \boldsymbol{e}, \boldsymbol{\lambda}) \tag{7}$$

$$0 = H_{\boldsymbol{u}}^T(t, \boldsymbol{x}, \boldsymbol{u}, \boldsymbol{\lambda}) \tag{8}$$

$$0 = H_{\boldsymbol{e}}^T(t, \boldsymbol{x}, \boldsymbol{e}, \boldsymbol{\lambda}) \tag{9}$$

and the boundary conditions for these differential equations are

$$t_0, \boldsymbol{x}_0 \text{ specified} \tag{10}$$

$$\psi(t_f, \boldsymbol{x}_f) = 0 \tag{11}$$

$$\Omega \triangleq \mathcal{L}_f + G_{\boldsymbol{x}_f}(\bar{\boldsymbol{f}}_f + \boldsymbol{e}_f) + G_{t_f} = 0 \tag{12}$$

$$\boldsymbol{\lambda}_f = G_{\boldsymbol{x}_f}^T(t_f, \boldsymbol{x}_f, \boldsymbol{\nu}) \tag{13}$$

A necessary condition for the optimality of the extremal controls is the Legendre–Clebsch condition, which checks the sign of the second derivative of the Hamiltonian with respect to the controls. For the normal controls to be minimal,

$$H_{\boldsymbol{uu}}(t, \boldsymbol{x}, \boldsymbol{u}, \boldsymbol{\lambda}) \geq 0$$

which can be checked only when the specific problem has been defined. However,

$$H_{\boldsymbol{ee}} = M^{-1}$$

so that the signs of the individual tuning parameters determine whether the EC controls minimize or maximize the performance index.

NE Controls

An NE path is a path that lies in the neighborhood of the optimal path and satisfies the first variation conditions.[4] The equations that describe this path are found by linearizing the optimality equations and boundary conditions about the optimal path. Even though it is not known whether the EC controls minimize or maximize the performance index, the NE path can be determined.

Linearizing Eqs. (6–9) about the optimal path produces the NE equations

$$\frac{\mathrm{d}(\tilde{\delta}\boldsymbol{x})}{\mathrm{d}t} = \bar{\boldsymbol{f}}_{\boldsymbol{x}}\tilde{\delta}\boldsymbol{x} + \bar{\boldsymbol{f}}_{\boldsymbol{u}}\tilde{\delta}\boldsymbol{u} + \tilde{\delta}\boldsymbol{e} \tag{14}$$

$$\frac{\mathrm{d}(\tilde{\delta}\boldsymbol{\lambda})}{\mathrm{d}t} = -H_{\boldsymbol{xx}}\tilde{\delta}\boldsymbol{x} - H_{\boldsymbol{xu}}\tilde{\delta}\boldsymbol{u} - H_{\boldsymbol{xe}}\tilde{\delta}\boldsymbol{e} - f_{\boldsymbol{x}}^T\tilde{\delta}\boldsymbol{\lambda} \tag{15}$$

$$0 = H_{\boldsymbol{ux}}\tilde{\delta}\boldsymbol{x} + H_{\boldsymbol{uu}}\tilde{\delta}\boldsymbol{u} + f_{\boldsymbol{u}}^T\tilde{\delta}\boldsymbol{\lambda} \tag{16}$$

$$0 = H_{\boldsymbol{ex}}\tilde{\delta}\boldsymbol{x} + H_{\boldsymbol{ee}}\tilde{\delta}\boldsymbol{e} + \tilde{\delta}\boldsymbol{\lambda} \tag{17}$$

where the substitutions $H_{\boldsymbol{x}\lambda} = \bar{\boldsymbol{f}}_{\boldsymbol{x}}^T$, $H_{\boldsymbol{u}\lambda} = \bar{\boldsymbol{f}}_{\boldsymbol{u}}^T$, and $H_{\boldsymbol{e}\lambda} = I$ (the identity matrix) have been made using the definition of the Hamiltonian, Eq. (5). For convenience, an augmented control vector is defined as $\bar{\boldsymbol{u}}^T = [\boldsymbol{u} \;\; \boldsymbol{e}]$. Equations (16) and (17) are rewritten more compactly as

$$0 = H_{\bar{\boldsymbol{u}}\boldsymbol{x}}\tilde{\delta}\boldsymbol{x} + H_{\bar{\boldsymbol{u}}\bar{\boldsymbol{u}}}\tilde{\delta}\bar{\boldsymbol{u}} + \bar{\boldsymbol{f}}_{\bar{\boldsymbol{u}}}^T\tilde{\delta}\boldsymbol{\lambda} \tag{18}$$

where

$$H_{\bar{\boldsymbol{u}}\boldsymbol{x}} = \begin{bmatrix} H_{\boldsymbol{ux}} \\ H_{\boldsymbol{ex}} \end{bmatrix}, \qquad \bar{\boldsymbol{f}}_{\bar{\boldsymbol{u}}}^T = \begin{bmatrix} \bar{\boldsymbol{f}}_{\boldsymbol{u}}^T \\ I \end{bmatrix}, \qquad H_{\bar{\boldsymbol{u}}\bar{\boldsymbol{u}}} = \begin{bmatrix} H_{\boldsymbol{uu}} & 0 \\ 0 & H_{\boldsymbol{ee}} \end{bmatrix}$$

The problem is now in the standard form, and the control perturbation is[4]

$$\tilde{\delta}\bar{\boldsymbol{u}} = -H_{\bar{\boldsymbol{u}}\bar{\boldsymbol{u}}}^{-1}\left\{\left[H_{\bar{\boldsymbol{u}}\boldsymbol{x}} + \bar{\boldsymbol{f}}_{\bar{\boldsymbol{u}}}^T(\bar{S} - \bar{R}\bar{Q}^{-1}\bar{R}^T)\right]\tilde{\delta}\boldsymbol{x} + \left[\bar{\boldsymbol{f}}_{\bar{\boldsymbol{u}}}^T\bar{R}\,\bar{Q}^{-1}\right]\delta\psi\right\} \tag{19}$$

where $\bar{S}$, $\bar{Q}$, and $\bar{R}$ are defined as

$$\bar{S} \triangleq S - (mm^T/\alpha) \tag{20}$$

$$\bar{Q} \triangleq Q - (nn^T/\alpha) \tag{21}$$

$$\bar{R} \triangleq R - (mn^T/\alpha) \tag{22}$$

The differential equations for the sweep variables are

$$\dot{S} = -SA - A^TS + SBS - C \tag{23}$$

$$\dot{R} = (SB - A^T)R \tag{24}$$

$$\dot{m} = (SB - A^T)m \tag{25}$$

$$\dot{Q} = R^TBR \tag{26}$$

$$\dot{n} = R^TBm \tag{27}$$

$$\dot{\alpha} = m^TBm \tag{28}$$

where the intermediate variables are defined as

$$A = \bar{\boldsymbol{f}}_{\boldsymbol{x}} - \bar{\boldsymbol{f}}_{\bar{\boldsymbol{u}}}H_{\bar{\boldsymbol{u}}\bar{\boldsymbol{u}}}^{-1}H_{\bar{\boldsymbol{u}}\boldsymbol{x}} \tag{29}$$

$$B = \bar{\boldsymbol{f}}_{\bar{\boldsymbol{u}}}H_{\bar{\boldsymbol{u}}\bar{\boldsymbol{u}}}^{-1}\bar{\boldsymbol{f}}_{\bar{\boldsymbol{u}}}^T \tag{30}$$

$$C = H_{\boldsymbol{xx}} - H_{\boldsymbol{x}\bar{\boldsymbol{u}}}H_{\bar{\boldsymbol{u}}\bar{\boldsymbol{u}}}^{-1}H_{\bar{\boldsymbol{u}}\boldsymbol{x}} \tag{31}$$

and the final values of these sweep variables are

$$\begin{aligned} S_f &= G_{\boldsymbol{x}_f\boldsymbol{x}_f}, & R_f &= \psi_{\boldsymbol{x}_f}^T, & m_f &= \Omega_{\boldsymbol{x}_f}^T \\ Q_f &= 0, & n_f &= \dot{\psi}_f, & \alpha_f &= \dot{\Omega}_f \end{aligned} \tag{32}$$

Hypersonic Glider Problem

A guidance law using EC is developed for a hypersonic glider. The optimal control goes to the ground, and the NE control is used to correct along-track and cross-track errors. This implementation of the NE control is different from the normal use and is explained in depth in a later section.

The differential equations that describe a nonthrusting vehicle moving over a nonrotating spherical Earth and modeled as a point mass are[7]

$$\frac{\mathrm{d}X}{\mathrm{d}t} = V\frac{r_s}{r_s + h}\cos\gamma\cos\chi \tag{33}$$

$$\frac{\mathrm{d}Y}{\mathrm{d}t} = V\frac{r_s}{r_s + h}\cos\gamma\sin\chi \tag{34}$$

$$\frac{\mathrm{d}h}{\mathrm{d}t} = V\sin\gamma \tag{35}$$

$$\frac{\mathrm{d}V}{\mathrm{d}t} = -\frac{D}{m_0} - g_s\left(\frac{r_s}{r_s + h}\right)^2\sin\gamma \tag{36}$$

$$\frac{\mathrm{d}\gamma}{\mathrm{d}t} = \frac{L}{m_0V} + \left[\frac{V}{r_s + h} - \frac{g_s}{V}\left(\frac{r_s}{r_s + h}\right)^2\right]\cos\gamma \tag{37}$$

$$\frac{\mathrm{d}\chi}{\mathrm{d}t} = \frac{S}{m_0V\cos\gamma} + \frac{V\cos\gamma\cos\chi}{r_s + h}\tan\left(\frac{Y}{r_s}\right) \tag{38}$$

The mean radius of the Earth and gravity at the Earth's surface have the numerical values

$$r_s = 20{,}925{,}672\ \text{ft}, \qquad g_s = 32.172\ \text{ft/s}^2$$

The glider has the mass and reference surface area

$$m_0 = 15.52\ \text{slugs}, \qquad S_R = 1.5\ \text{ft}^2$$

The aerodynamic lift, drag, and side force are written in terms of nondimensional coefficients as

$$L = \tfrac{1}{2}\rho V^2 S_R C_L, \qquad D = \tfrac{1}{2}\rho V^2 S_R C_D, \qquad S = \tfrac{1}{2}\rho V^2 S_R C_S$$

respectively, where the air density ρ is determined from interpolated data of the 1976 standard atmosphere.[8] The aerodynamic coefficients are determined by linear interpolation of wind-tunnel data that are stored as a function of angle of attack, sideslip angle, Mach number, and Reynolds number.

Approximate Model

The preceding equations of motion define the simulation environment (or truth model) that describes the glider. Because they are highly nonlinear, a reduction to a set of approximate equations must be performed to get an analytical solution for the optimal controls. The following approximations are used.

1) *Low-altitude flight*: The altitude of the glider is small compared with the radius of the Earth, and so, $r_s + h \cong r_s$.

2) *Parabolic drag polar*: The glider is assumed to be flying hypersonically throughout the trajectory, and so, the nondimensional drag coefficient is approximated by

$$C_D \cong C_{D_0}\left(1 + \bar{C}_L^2 + \bar{C}_S^2\right)$$

where $\bar{C}_L \triangleq C_L / C_L^*$ and $\bar{C}_S \triangleq C_S / C_L^*$ are the scaled lift and side-force coefficients and are the aerodynamic controls for this problem. The drag polar constants are

$$C_{D_0} = 0.043, \qquad C_L^* = 0.2888$$

and the maximum lift-to-drag ratio is $E^* = 3.281$.

3) *Dominant aerodynamic forces*: Because the glider is flying hypersonically, the aerodynamic forces are assumed to be much larger than the other terms in the V, γ, and χ differential equations.

4) *Exponential density*: An analytical approximation for the air density is

$$\rho \cong \rho_s e^{-h/h_R} \tag{39}$$

where $\rho_s = 0.0023769\ \text{slug/ft}^3$ is the density at sea level and $h_R = 23{,}800$ ft is the density scale height chosen by fitting an exponential curve to a plot of density vs altitude.

5) *Linearized flight-path angle*: The flight-path angle is linearized about the current flight-path angle γ_0, which simplifies the trigonometric functions to

$$\sin\gamma \cong a_0 + a_1\gamma \qquad \cos\gamma \cong b_0 + b_1\gamma \qquad 1/\cos\gamma \cong c_0 + c_1\gamma$$

where a_i, b_i, and c_i are the series expansion coefficients. The accuracy of these approximations improves toward the end of the trajectory when the flight-path angle changes less.

The two major differences between the approximations used here and those used in Ref. 5 are as follows: 1) Loh's approximation[9] is not used to simplify the differential equation for the flight-path angle and 2) linearization about $\gamma = 0$ was used in Ref. 5, whereas linearization about the current flight-path angle is used here.

The dimensional states (X, Y, h, V) are replaced with the following nondimensional variables:

$$\xi \triangleq \frac{X}{h_R}, \qquad \eta \triangleq \frac{Y}{h_R}$$

$$w \triangleq \frac{C_L^* S_R h_R}{2m_0}\rho(h), \qquad v \triangleq \ln\left(\frac{V^2}{g_s r_s}\right)$$

and the differential equation for the nondimensional density replaces Eq. (35). In addition, the time derivative of a new integration variable z is defined as[1]

$$\frac{dz}{dt} \triangleq \frac{Vw}{h_R}$$

The value of z increases along any trajectory because its time derivative is always positive; the initial value of z is chosen to be 0. For the initial conditions of the problem that is solved later, γ could be used as the variable of integration[5]; in general this is not the case.

If the approximate dynamics are added and subtracted from the right-hand sides, the state differential equations (33–38) can be written as

$$\frac{d\xi}{dz} = \frac{(b_0 + b_1\gamma)\cos\chi}{w} + e_\xi \tag{40}$$

$$\frac{d\eta}{dz} = \frac{(b_0 + b_1\gamma)\sin\chi}{w} + e_\eta \tag{41}$$

$$\frac{dw}{dz} = -(a_0 + a_1\gamma) + e_w \tag{42}$$

$$\frac{dv}{dz} = -\frac{\left(1 + \bar{C}_L^2 + \bar{C}_S^2\right)}{E^*} + e_v \tag{43}$$

$$\frac{d\gamma}{dz} = \bar{C}_L + e_\gamma \tag{44}$$

$$\frac{d\chi}{dz} = c_0\bar{C}_S + e_\chi \tag{45}$$

where the six EC controls e_ξ, e_η, e_w, e_v, e_γ, and e_χ replace the small terms.

Guidance Scheme

A close examination of the model equations reveals that the last four equations are linear in the states (quadratic in the aerodynamic controls). However, the range equations (40) and (41) contain the state w in the denominator. An analytical optimal control solution for the descent to a constrained downrange, cross range, and altitude cannot be found because of this nonlinearity.

For this reason, the guidance scheme from Ref. 5 is used. At each guidance step:

1) The linearization coefficients ($a_0, \ldots, c_1$) are recalculated on the basis of the current state of the glider.

2) The unconstrained-range (UR) optimal controls are calculated for a descent from the current position to the constrained final altitude only.

3) The final states of the glider using the UR controls are determined by quadrature integration of the necessary model differential equations.

4) As shown Fig. 1, the initial state perturbation is zero ($\tilde{\delta}\mathbf{x} = 0$), and so, the miss distance between the desired final position and the UR final location ($\delta\psi$) is used to calculate the NE controls. The NE corrections are added to the UR controls and applied to the vehicle.

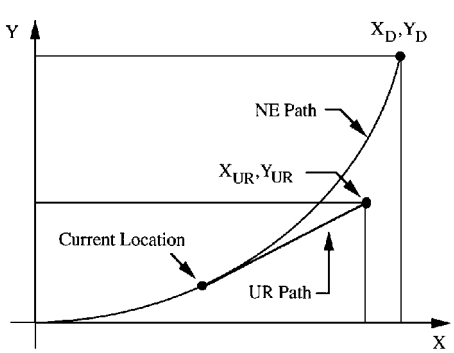

Fig. 1 Neighboring optimal miss distances.

Optimal UR Controls

The optimal control problem is to find the two sets of controls $\boldsymbol{u}$ and $\boldsymbol{e}$ that, respectively, minimize and extremize the performance index

$$J = \left[-v_f + \frac{1}{2} \int_o^{z_f} e^T M^{-1} e \, \mathrm{d}z \right]$$

subject to the model differential equations (40–45), and the boundary conditions

$$z_0 = 0, \qquad \boldsymbol{x}_0 \text{ specified}, \qquad \psi(z_f, \boldsymbol{x}_f) = \begin{bmatrix} \xi_f - \xi_D \\ \eta_f - \eta_D \\ w_f - w_D \end{bmatrix} = 0$$

where the subscript D denotes the desired final location. The performance index is separable for this problem because $\mathrm{d}v/\mathrm{d}z = f_1(\boldsymbol{u}) + f_2(e)$ and integration is a linear operator. The Bolza function and the Hamiltonian for this problem are

$$G = -v_f + \nu_\xi(\xi_f - \xi_D) + \nu_\eta(\eta_f - \eta_D) + \nu_w(w_f - w_D) \quad (46)$$

$$\begin{aligned} H = {} & \frac{1}{2}\left[\frac{e_\xi^2}{M_\xi} + \frac{e_\eta^2}{M_\eta} + \frac{e_w^2}{M_w} + \frac{e_v^2}{M_v} + \frac{e_\gamma^2}{M_\gamma} + \frac{e_\chi^2}{M_\chi} \right] \\ & + \lambda_\xi \left[\frac{(b_0 + b_1\gamma)\cos\chi}{w} + e_\xi \right] + \lambda_\eta \left[\frac{(b_0 + b_1\gamma)\sin\chi}{w} + e_\eta \right] \\ & + \lambda_w[-(a_0 + b_0\gamma) + e_w] + \lambda_v \left[-\frac{\left(1 + \bar{C}_L^2 + \bar{C}_S^2\right)}{E^*} + e_v \right] \\ & + \lambda_\gamma[\bar{C}_L + e_\gamma] + \lambda_\chi[f_0\bar{C}_S + e_\chi] \end{aligned} \quad (47)$$

The downrange and cross-range equations and constraints are not needed for the calculation of the UR controls. However, they must be included in the problem formulation for the subsequent calculation of the NE controls. Therefore, for the calculation of the UR controls, ξ_D and η_D are set equal to ξ_{UR} and η_{UR} and the Lagrange multipliers ν_ξ, ν_η, λ_ξ, and λ_η become zero.[5] From Eqs. (7) and (13), the other multipliers are

$$\lambda_w = \text{unknown constant}, \qquad \lambda_v = -1$$
$$\lambda_\gamma = a_1\lambda_w(z - z_f), \qquad \lambda_\chi = 0$$

The extremal UR controls are determined from Eqs. (8) and (9) to be

$$\bar{C}_{L_{\mathrm{UR}}} = -(E^*/2)a_1\lambda_w(z - z_f) \quad (48)$$

$$\bar{C}_{S_{\mathrm{UR}}} = 0 \quad (49)$$

$$e_\xi = e_\eta = e_\chi = 0 \quad (50)$$

$$e_w = -\lambda_w M_w \quad (51)$$

$$e_v = M_v \quad (52)$$

$$e_\gamma = -a_1\lambda_w M_\gamma(z - z_f) \quad (53)$$

using the expression for λ_γ given earlier. Both $\bar{C}_S$ and e_χ are zero, which implies that the UR descent occurs in a vertical plane. The aerodynamic controls satisfy the Legendre–Clebsch condition because

$$H_{\boldsymbol{uu}} = \begin{bmatrix} -2\lambda_v/E^* & 0 \\ 0 & -2\lambda_v/E^* \end{bmatrix}$$

is positive definite.

The unknowns λ_w and z_f are determined by analytically integrating Eq. (44), integrating Eq. (42), and applying the first integral.[10] The expression for λ_w in terms of z_f is

$$\lambda_w = \frac{d_1 + \sqrt{d_1^2 - 2K_v d_2}}{d_2}$$

where

$$d_1 \triangleq a_0 + a_1\gamma_0, \qquad d_2 \triangleq -M_w - a_1^2 K_\gamma z_f^2$$

and the constants K_v and K_γ are defined as

$$K_v \triangleq (1/E^*) + (M_v/2), \qquad K_\gamma \triangleq M_\gamma - (E^*/2)$$

The value of z_f is a root of the sixth-order polynomial

$$p_6 z_f^6 + p_4 z_f^4 + p_3 z_f^3 + p_2 z_f^2 + p_0 = 0 \quad (54)$$

whose coefficients are

$$p_6 = 8a_1^4 K_v K_\gamma^2$$

$$p_4 = 48a_1^2 M_\omega K_v K_\gamma - 12K_\gamma\left[a_1^4\gamma_0^2 + a_0^2 a_1^2 + 2a_0 a_1^3\gamma_0\right]$$

$$p_3 = -48K_\gamma\Delta\,\omega\left[a_1^3\gamma_0 + a_0 a_1^2\right]$$

$$p_2 = 72K_v M_\omega^2 - 36a_1^2 K_\gamma\Delta\,\omega^2 + 36M_\omega\left[a_1^2\gamma_0^2 + 2a_0 a_1\gamma_0 + a_0^2\right]$$

$$p_0 = -36\Delta\,\omega^2 M_\omega$$

Simulation work reveals that the correct value of z_f is the second positive root of Eq. (54). This value must be determined numerically because there is no known analytical solution to a sixth-order polynomial.

NE Controls

The NE trajectory is defined relative to the UR path. Therefore, all of the partial derivatives and sweep variables used for the NE control computation are evaluated on the extremal path along which $p_\xi = p_\eta = 0$. The UR trajectory is recomputed at each sample point for this problem, and so, the glider always starts on the UR trajectory at $z_0 = 0$. The initial state perturbation is therefore zero ($\delta\boldsymbol{x}_0 = 0$), and the NE control reduces to

$$\delta\boldsymbol{u}_0 = -\left[H_{\boldsymbol{uu}}^{-1} f_{\boldsymbol{u}}^T \bar{R}\,\bar{Q}^{-1}\right]_0 \delta\psi$$

where the perturbed final constraint manifold is

$$\delta\psi = \psi_{\boldsymbol{x}_f}\delta\boldsymbol{x}_f = \begin{bmatrix} \xi_D - \xi_f \\ \eta_D - \eta_f \\ 0 \end{bmatrix}$$

This form for the NE controls is valid only because the controls are held constant over each guidance interval.

The boundary conditions for the sweep variables are determined from Eq. (32) to be

$$S_f = 0_{6\times 6}, \qquad Q_f = 0_{6\times 6}, \qquad \alpha_f = 0$$

$$R_f = \begin{bmatrix} 1 & 0 & 0 \\ 0 & 1 & 0 \\ 0 & 0 & 1 \\ 0 & 0 & 0 \\ 0 & 0 & 0 \\ 0 & 0 & 0 \end{bmatrix}, \qquad m_f = \begin{bmatrix} 0 \\ 0 \\ 0 \\ 0 \\ -a_1\lambda_w \\ 0 \end{bmatrix}$$

$$n_f = \begin{bmatrix} \dfrac{(b_0 + b_1\gamma_f)\cos\chi_f}{w_f} \\ \dfrac{(b_0 + b_1\gamma_f)\sin\chi_f}{w_f} \\ -(a_0 + a_1\gamma_f) - \lambda_w M_w \end{bmatrix}$$

These final conditions are used to integrate the differential equations describing the sweep variables backward from z_f to $z_0 \triangleq 0$.

The differential equation for S is homogeneous because $C = 0_{6\times 6}$. Therefore, because S_f is zero, $S(z) = 0_{6\times 6}$. The derivative

of the R matrix is defined in Eq. (24). Solving for those elements of R that can be integrated yields

$$R(z) = \begin{bmatrix} 1 & 0 & 0 \\ 0 & 1 & 0 \\ R_{31} & R_{32} & 1 \\ 0 & 0 & 0 \\ R_{51} & R_{52} & a_1(z - z_f) \\ R_{61} & R_{62} & 0 \end{bmatrix}$$

The remaining elements have the following differential equations:

$$\frac{dR_{31}}{dz} = \frac{(b_0 + b_1\gamma)\cos\chi}{w^2}, \qquad \frac{dR_{32}}{dz} = \frac{(b_0 + b_1\gamma)\sin\chi}{w^2}$$

$$\frac{dR_{51}}{dz} = \frac{-b_1\cos\chi}{w} + a_1 R_{31}, \qquad \frac{dR_{52}}{dz} = \frac{-b_1\sin\chi}{w} + a_1 R_{32}$$

$$\frac{dR_{61}}{dz} = \frac{(b_0 + b_1\gamma)\sin\chi}{w}, \qquad \frac{dR_{62}}{dz} = \frac{-(b_0 + b_1\gamma)\cos\chi}{w}$$

The differential equations for the first five elements of Q are

$$\frac{dQ_{11}}{dz} = M_\xi + R_{31}^2 M_w + K_\gamma R_{51}^2 + K_\chi R_{61}^2$$

$$\frac{dQ_{12}}{dz} = R_{31}R_{32}M_w + K_\gamma R_{51}R_{52} + K_\chi R_{61}R_{62}$$

$$\frac{dQ_{13}}{dz} = R_{31}M_w + a_1 K_\gamma R_{51}(z - z_f)$$

$$\frac{dQ_{22}}{dz} = M_\eta + R_{32}^2 M_w + K_\gamma R_{52}^2 + K_\chi R_{62}^2$$

$$\frac{dQ_{23}}{dz} = R_{32}M_w + a_1 K_\gamma R_{52}(z - z_f)$$

where

$$K_\chi \triangleq M_\chi + c_0^2(E^*/2)$$

The last diagonal element of Q is integrated to be

$$Q_{33}(z) = M_w(z - z_f) + a_1^2 K_\gamma\left[(z^3/3) - z_f z^2 + z_f^2 z - \left(z_f^3/3\right)\right]$$

The m matrix is constant, and $m(z) = m_f$. The derivatives of the first two elements of the n matrix are

$$\frac{dn_1}{dz} = -a_1 K_\gamma \lambda_w R_{51}, \qquad \frac{dn_2}{dz} = -a_1 K_\gamma \lambda_w R_{52}$$

and the third element of the matrix is

$$n_3(z) = -a_1^2 K_\gamma \lambda_w\left[(z^2/2) - z_f z + \left(z_f^2/2\right)\right] - (a_0 + a_1\gamma_f) - \lambda_w M_w$$

Finally, the sweep variable α is

$$\alpha(z) = a_1^2 K_\gamma \lambda_w^2 (z - z_f)$$

The sweep variables are used to calculate the NE control perturbations from Eq. (20). The 13 differential equations for the matrix elements that are listed must be integrated numerically (with either Runge–Kutta or cascaded quadrature).

Numerical Results

The NE corrections are added to the UR optimal controls to obtain the total aerodynamic controls

$$\bar{C}_L = -(E^*/2)a_1\lambda_w(z - z_f) + \tilde{\delta}\bar{C}_L \tag{55}$$

$$\bar{C}_S = \tilde{\delta}\bar{C}_S \tag{56}$$

which are applied to the vehicle. These commanded controls are assumed to be instantaneously achievable. At each guidance step during the simulation (every 0.1 s), the linearization coefficients and the controls are computed and held constant until the next guidance step. The simulations performed here show feasibility of this method and no effort has been made to minimize computation times. However, both the guidance law and a nonlinear three-degree-of-freedom simulation (coded in Fortran) run faster than real time on a DEC 5000 workstation.

Neither the EC controls nor their NE perturbations enter directly in the simulation environment because they do not appear explicitly in the simulation equations of motion. However, they are included implicitly throughout the problem in the equation for p_ω, the equations for the coefficients $a_0, a_2, \ldots, a_6$, and the NE sweep variable differential equations.

The glider is initially flying at a constant altitude of 100,000 ft with a flight-path angle of 0 deg. The initial velocity of the vehicle is 11,000 ft/s and both the initial time and downrange are set to zero. Depending on the values of the tuning parameters, the UR trajectory to a final altitude of 0 ft ends at a downrange of about 70 nm and exactly no cross range. The first scenario that is examined is the descent to a downrange of 70 nm and a cross range of 10 nm.

Four control laws are used to guide the vehicle. The first two are Eqs. (55) and (56) with different values of the tuning parameters. The untuned controller has all of the tuning parameters set to zero. This control law is similar to the control law of Ref. 5 except for the approximations made in the dynamics. The tuned controller uses a suboptimal set of tuning parameters chosen by testing various combinations of parameter values. The only parameters changed from zero for this tuned set are $M_\omega = 1/500$ and $M_v = 1$. The positive M imply that this is a min-min problem and not a min-max problem, which would be expected from a differential game formulation.[6] In other words, both the aerodynamic controls and the two EC controls are chosen to maximize the final velocity of the glider.

The third control law is a seven-node piecewise-linear control law determined by a numerical parameter optimization code[11] that uses the true vehicle dynamics. The last control law is a proportional navigation (PRONAV) scheme that weights the final miss distance 10 times more than the integrated square control effort.[10]

Unfortunately, the determinant of the sweep variable $\bar{Q}$ decreases tremendously along the trajectory for both sets of the tuning parameters (see Fig. 2). The small determinant causes the NE control corrections to get very large, because they are a function of $\bar{Q}^{-1}$. To avoid the misleading large decrease in the final velocity due to large terminal controls, PRONAV is used in place of the tuned and untuned control laws after the glider passes 10,000-ft altitude, which corresponds roughly to the last 2 s of the trajectory. The switch to PRONAV is justified by the fact that the glider is essentially pointing directly at the desired final position at 10,000-ft altitude and very little control effort is needed to achieve the desired final position.

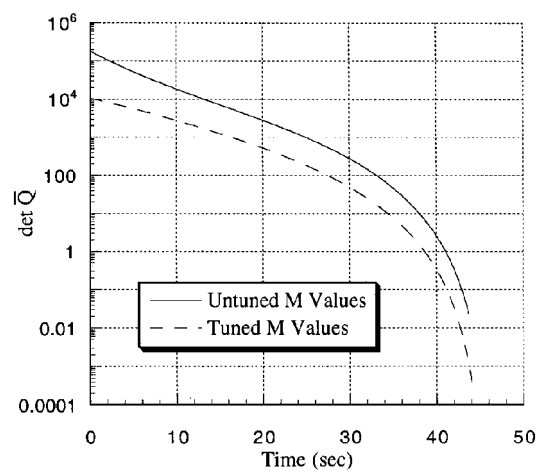

Fig. 2 Determinant of the sweep variable $\bar{Q}$.

Table 1 Performance comparison of the controllers for X_D = 70 nm, Y_D = 10 nm

Controller	V_f, ft/s
Untuned	6517.6
Tuned	6780.4
Numerical optimal	6798.7
PRONAV	4767.0

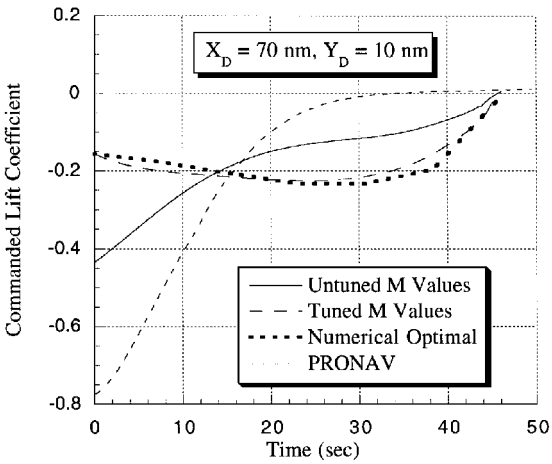

Fig. 3 Comparison of commanded C_L.

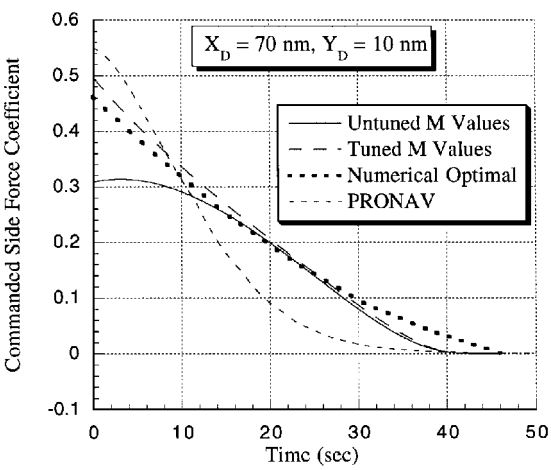

Fig. 4 Comparison of commanded C_S.

The commanded lift and side-force coefficients generated by the four control laws are compared in Figs. 3 and 4. For both the lift and the side force, the tuning procedure modifies the controls to be more like the numerically determined optimal control. The tuned side-force coefficient does not match the numerical optimal control as well as the lift coefficient because the cross-range control is achieved only by the NE control.

All of the control laws successfully guide the vehicle to the desired final location. The trajectories that the glider follows using these control laws are shown in Figs. 5 and 6 and the final velocities of the glider are listed in Table 1. PRONAV yields the lowest final velocity, which is to be expected because it minimizes the miss distance (relative to the control effort) and does not maximize the final velocity. For the controller derived in this paper, the tuning procedure increases the final velocity over 250 ft/s. In addition, the final velocity using the tuned controller is within 20 ft/s of the velocity produced using the numerical optimal control law.

The altitude profile of the glider using the tuned control law is almost coincident with the numerically determined profile. However, the ground tracks using the tuned and untuned controllers are

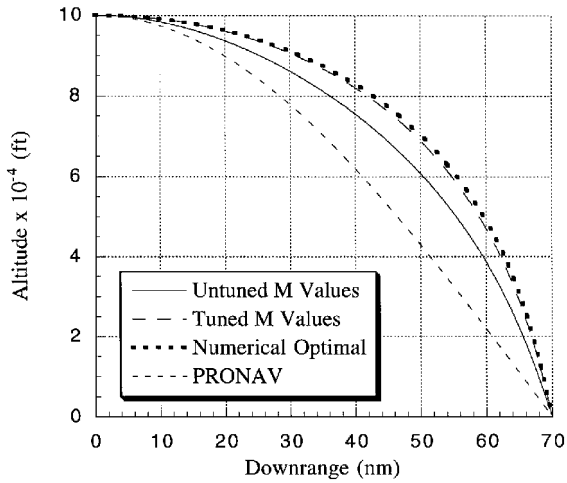

Fig. 5 Altitude profiles for the controllers.

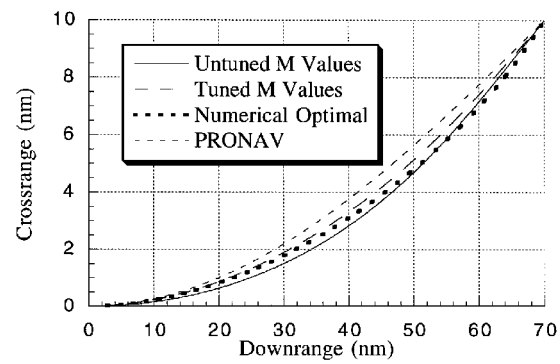

Fig. 6 Ground tracks for the four controllers.

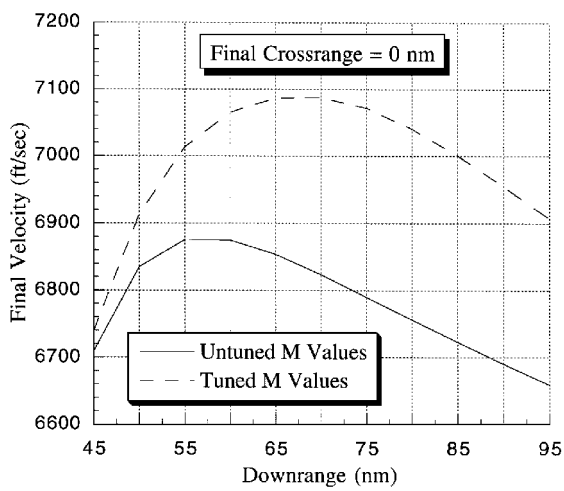

Fig. 7 Performance comparisons for downranges.

equally far from the ground track produced using the numerical optimal control law. This situation arises because the UR optimal side-force control is identically zero and the cross range is achieved solely with the NE control. The tuning procedure is therefore more effective when the UR control has a specific form about which the NE controls can be linearized.

A comparison of the tuned and untuned control laws for different desired final locations is shown in Figs. 7 and 8. Both controllers guide the vehicle to the desired final locations and the tuned controller consistently outperforms the untuned controller. The performance gain of the tuned controller does decrease as the final position gets farther from the design point about which the parameters were tuned.

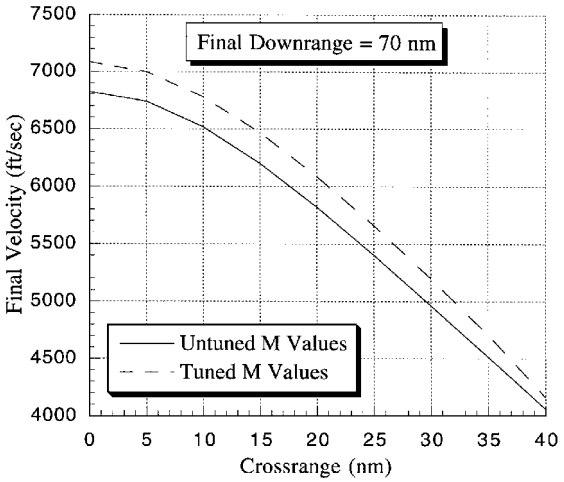

Fig. 8 Performance comparisons for cross ranges.

Conclusions

The NE controls are derived for a system that includes EC controls to simplify the model equations of motion. The tuning parameters associated with the EC controls are adjusted after the NE controls are added to the optimal controls and simulated on a computer. The specific example shows that the performance of the tuned control law approaches the performance achieved using a numerically determined piecewise-linear controller and is much better than the performance obtained using a proportional navigation control law.

Acknowledgments

This work was supported in part by the U.S. Department of Energy under Contract DE-AC04-94AL-85000. Sandia National Laboratories is a multiprogram laboratory operated by Sandia Corporation, a Lockheed Martin company, for the U.S. Department of Energy.

References

[1]Speyer, J. L., and Crues, E. Z., "Approximate Optimal Atmospheric Guidance Law for Aeroassisted Plane-Change Maneuvers," *Journal of Guidance, Control, and Dynamics*, Vol. 13, No. 5, 1990, pp. 792–802.

[2]Kim, T. J., and Hull, D. G., "Optimal Control Design Using Error Compensation," *Recent Trends in Optimization Theory and Applications*, edited by R. P. Agarwal, World Scientific, Maplewood, NJ, 1995, pp. 193–206.

[3]Muzumdar, D. V., and Hull, D. G., "Midcourse Guidance for a Short Range Attack Missile Using Error Compensation," *Proceedings of the AIAA Guidance, Navigation, and Control Conference* (Baltimore, MD), AIAA, Washington, DC, 1995.

[4]Bryson, A. E., and Ho, Y. C., *Applied Optimal Control,* Hemisphere, New York, 1975.

[5]Eisler, G. R., and Hull, D. G., "Guidance Law for Hypersonic Descent to a Point," *Journal of Guidance, Control, and Dynamics*, Vol. 17, No. 4, 1994, pp. 649–654.

[6]Isaacs, R., *Differential Games,* Krieger, Malabar, FL, 1975.

[7]Feeley, T. S., and Speyer, J. L., "A Real-Time Approximate Optimal Guidance Law for Flight in a Plane," *Proceedings of the 1990 American Control Conference* (San Diego, CA), American Automatic Control Council, Green Valley, AZ, 1990.

[8]Anon., *U.S. Standard Atmosphere*, U.S. Committee on Extension to the Standard Atmosphere, U.S. Government Printing Office, Washington, DC, 1976.

[9]Loh, W. H. T., *Dynamics and Thermodynamics of Planetary Entry,* Prentice–Hall, Englewood Cliffs, NJ, 1963.

[10]Kim, T. J., "A Mixed Nonlinear/Linear Control Design for Optimal Descent Trajectories," Ph.D. Thesis, Dept. of Aerospace Engineering and Engineering Mechanics, Univ. of Texas, Austin, TX, 1994.

[11]Lasdon, L. S., and Waren, A. D., *GRG2 User's Guide,* Dept. of Management Sciences and Information Systems, Univ. of Texas, Austin, TX, July 1994.